

## Endothelialization of Titanium Surfaces\*\*

By Steven R. Meyers, Paul T. Hamilton, Elisabeth B. Walsh, Daniel J. Kenan,\* and Mark W. Grinstaff\*

In the extracellular matrix (ECM), chemical cues are present that control all aspects of cell biology.<sup>[1–3]</sup> These surface-bound and soluble factors provide the necessary adhesion and signaling for normal cellular activity, and without such matrix support, the cells will quickly apoptose. Implanted device surfaces lack the molecular features that provide guidance to the surrounding cells to afford optimal *in vivo* integration and function. One class of implanted materials are metal implants, which are commonly used in cardiovascular therapy (e.g., stents) and orthopedic procedures (e.g., hip replacement). While such materials are favored for their inertness and mechanical strength, negative consequences can arise from suboptimal tissue integration. For example, during a coronary angioplasty an occluded coronary artery is opened using a balloon catheter and then a metal stent is inserted to provide a permanent framework supporting vascular patency. If the artery re-occludes due to smooth muscle cell proliferation, in a process called restenosis, a second procedure is required to re-establish blood flow. Restenosis used to occur in about 25 % of patients, but with the introduction of stents that elute a mitotic inhibitor, such as paclitaxel, this number has been reduced significantly.<sup>[4]</sup> However, there is new concern regarding the use of drug-eluting stents owing to an increased thrombolytic potential of two to three fold compared to bare metal stents.<sup>[5]</sup> An alternative approach to the use of drugs would be to develop materials that better integrate with the surrounding endothelial cells that line the artery to afford a

prohealing response. Ideally, such materials would provide cues to appropriately direct cellular activity, for example, through integrin interactions that control an assortment of biological processes.<sup>[6,7]</sup> In order to impart suitable extracellular signals, we are developing interfacial coatings to study and ultimately control cell biology on a metal implant. As our first foray into this area, we have synthesized a procellular coating that adheres to a Ti surface under mild aqueous conditions and retains endothelial cells under flow.

In its simplest form this interfacial coating is a 20 to 30-mer peptide that possesses two domains, one that binds to Ti metal and a second domain that binds to endothelial cells (Fig. 1). As such, this interfacial peptide is modular by design and the domains can be interchanged based on the specific material to

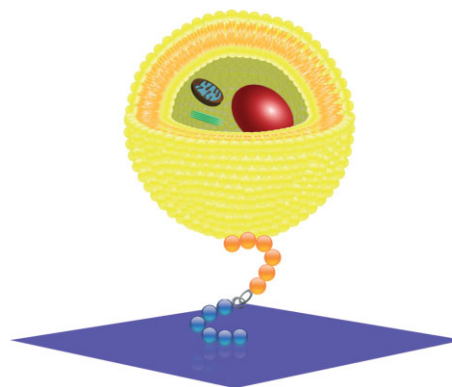


**Figure 1.** Schematic of an interfacial coating residing at the boundary between a material and a cell. Blue residue positions represent the material-binding domain, while orange represents those residues that bind the cell.

[\*] Prof. D. J. Kenan  
Department of Pathology, Duke University Medical Center  
Durham, NC 27710 (USA)  
E-mail: kenan001@mc.duke.edu

Prof. M. W. Grinstaff, S. R. Meyers  
Departments of Biomedical Engineering and Chemistry, Boston  
University  
Boston, MA 02215 (USA)  
E-mail: mgrin@bu.edu

Dr. P. T. Hamilton  
Affinergy, Inc.  
Durham, NC 27713 (USA)

E. B. Walsh  
Department of Chemistry, Duke University  
Durham, NC 27708 (USA)

[\*\*] M. W. G. and D. J. K. would like to thank the NIH for funding (R01-EB-000501). We thank the team at Affinergy Inc. for useful discussions, especially Dr. Greg Harbers for performing XPS studies, the technical staff at the Shared Materials Instrumentation Facility at Duke University for useful technical advice, and Xiaojuan Khoo of BU for the Ti coated glass slides. S. R. M. would like to thank the NIH Training Program in Quantitative Biology and Physiology at Boston University.

be used. For this set of experiments, the ubiquitous arginine–glycine–aspartic acid (RGD) integrin-binding motif was selected for the cell-binding domain. This tripeptide sequence, found on most ECM proteins, readily binds to a number of cell types, including endothelial cells. Specific endothelial cell-binding peptides have yet to be reported, although the identification of cell distinctive peptides is an active research area with some recent notable successes (e.g., neutrophils, hematopoietic stem cells, cancer cells).<sup>[8–11]</sup> Previous efforts to attach the RGD domain to Ti surfaces have typically required careful control over the multistep process required to coat the material.<sup>[12–18]</sup> Our next step was to identify peptide sequences that bind Ti metal. We chose to use a phage display combinatorial library that operates through affinity selection of phage-

encoded peptides to identify the binding motif(s).<sup>[19–22]</sup> This iterative selection process has been used previously to isolate peptides that recognize a variety of diverse targets such as GaAs nanocrystals, iron oxide, gold, polystyrene, and a variety of other materials.<sup>[23–37]</sup>

A filamentous M13 phage displaying a 19-mer peptide (SCX<sub>16</sub>C, where the one letter abbreviations for the amino acids are used and X represents one of the twenty amino acids encoded by synthetic NNK (N: A, C, G, T; K: G, T) codons, 10<sup>10</sup> total phage screened, 10<sup>8</sup> complexity) attached to the amino terminus of the pIII coat protein was used to identify peptides that adhere to 6Al-4V Ti, a commonly used implant material. Our prior experiences with the commercial libraries have not yielded adequate binders to our previous targets, and thus we have designed new libraries such as the one used in these experiments. This library was designed to have one fixed cysteine residue in its sequence to favor the possibility of a cyclic disulfide motif being selected due to the reduced entropic penalty associated with binding. The phage that bound to the target Ti substrate were eluted and amplified by infection of a bacterial host. Once the target binding phage clones were identified, the base sequence of the DNA insert in the phage genome was located and then translated to yield the corresponding amino acid sequence displayed on the phage surface. After three rounds of screening, we identified 10 peptides with high Ti affinity, listed in Table 1. Sequence **4**, SCSDCLKSVDIFIPSSLASS, was selected for further study because its relative binding affinity on phage was two to four

**Table 1.** Ti binding sequences isolated from the phage display combinatorial library and their functionalized derivatives. Italicized residues indicate nonvariable positions.

#	Sequence	#	Sequence
1	SCFWFLRWSLFIVLFTCCS	8	SCSENFMFNMYGTGVCTES
2	SCESVDCFADSRMAKVMSM	9	SCSSFVSEMFCAVSSYS
3	SCVGFFCITGSDVASVNSS	10	SCGLNFPLCSFVDFQAQDAS
4	SCSDCLKSVDIFIPSSLASS	11	SCSDCLKSVDIFIPSSLASS-SSG-Biotin
5	SCAFDCPSSVARSPGEWSS	12	SCSDCLKSVDIFIPSSLASS-SSG-RGDSP
6	SCMLFSSVDFCGMLISDLS	13	SCSDCLKSVDIFIPSSLASS-SSG-RGESP
7	SCVDYVMHADSPGPDGLNS		

fold greater than the weakest binders. Previous experiments have suggested that this initial screen is an effective method to rapidly quantify the relative binding strengths of the sequences without having to fully synthesize them.<sup>[36]</sup> Analysis of the 10 sequences shows that D occurs more frequently than expected (13 occurrences, 5.2 expected in 160 library-encoded residues, ratio of 2.5 times over expected), and that C and S are slightly enriched in the variable region (10 occurrences, 5.2 expected, ratio of 1.9 and 27 occurrences, 15.5 expected, ratio of 1.7 times over expected, respectively). This suggests a possible mode of coordination to the Ti oxide surface via hydrogen bonding for this peptide sequence. Finally, F is highly enriched (18 occurrences, 5.2 expected, ratio of 3.5 over ex-

pected), although the other aromatic residues are not (see Fig. S2 in the Supporting Information).

Next, peptide **4** was prepared using automated solid-phase peptide synthesis following standard *N*-9-fluorenylmethoxycarbonyl (Fmoc) protocols containing either a C-terminal biotin, the prototypical RGD integrin-binding domain, or the closely related, but nonfunctional arginine–glycine–glutamic acid (RGE). The resulting peptides: SCSDCLKSVDIFIPSSLASS-SSG-Biotin, **11**, SCSDCLKSVDIFIPSSLASS-SSG-RGDSP, **12**, and SCSDCLKSVDIFIPSSLASS-SSG-RGESP, **13**, contained a tripeptide spacer of SSG to separate the Ti binding domain from the biotin, RGD, or RGE domain. We coated Ti disks (height = 3.8 mm; diameter = 12.7 mm), which were lathe cut from a 6Al-4V Ti rod (root mean square ≈ 150 nm), by dissolving **12** and **13** in aqueous buffer, and applying the solutions to the disk surfaces followed by washings to remove nonspecific binding. The disk surface was cleaned extensively prior to use and was characterized using atomic force microscopy (AFM), scanning electron microscopy (SEM), and X-ray photoelectron spectroscopy (XPS). The latter confirmed the presence of a TiO<sub>2</sub> coating (Ti2p/O1s = 0.27 ± 0.003) as well as some vanadium and aluminum as expected, with values similar to those reported in the literature.<sup>[38]</sup> Prior to application the contact angle of the Ti surface was 53.4° ± 2.0°, which is in agreement with literature values for bulk Ti6Al4V materials where depending on the surface roughness the angle can vary from 35° to 75°C.<sup>[39]</sup> After coating with **12** the contact angle decreased to 37.3° ± 1.4° (*n* = 3; *p* < 5 × 10<sup>-3</sup>), with a similar decrease to 38.4° ± 1.5° recorded for **13**. As a control, a coating of bovine serum albumin (BSA) did not change the contact angle of the Ti significantly (53.9° ± 3.8°; *p* = 0.84). We next determined the binding affinity of **11** to Ti by enzyme-linked immunosorbent assay (ELISA) using a streptavidin-horseradish peroxidase conjugate and a 2,2'-azino-bis(3-ethylbenzthiazoline-6-sulfonic acid) (ABTS) readout. The affinity constant (*k*<sub>aff</sub>) of the peptide material domain to the Ti disk was found to be 4.1 × 10<sup>6</sup> M<sup>-1</sup>.

To assess the ability of the Ti-RGD macromolecule, **12**, to affect endothelial biology on a Ti metal surface, we examined attachment morphology, proliferation, and cell binding. As a first step in the process, optical images of human umbilical vein endothelial cells (HUVECs) on a Ti surface were obtained by utilizing glass microscope coverslips coated with a 20 nm film of Ti metal (root mean square ≈ 0.75 nm). Due to the difficulty in evaporating alloys because of the differing vapor pressures of the components, commercially pure Ti was substituted as a model for these studies. XPS data again reveals the presence of TiO<sub>2</sub> (Ti2p/O1s = (0.48 ± 0.01)), however as expected, this data verifies that the oxide layer on pure Ti is not identical to the oxide layer seen on the Ti6Al4V alloy, but is similar to values reported in the literature.<sup>[40]</sup> Additionally, the XPS data shows complete Ti surface coverage as the Si2p peak is not significantly greater than that on the bulk Ti disks (*p* = 0.23). Next, we examined the binding affinity of the peptide to this new TiO<sub>2</sub> surface. Binding strength measure-

ments determined using the same procedure as previously used showed that the affinity constant was slightly lower but within the same order of magnitude as with the Ti disks. This suggests that the Ti binding peptide, **12**, has general micromolar affinity for TiO<sub>2</sub> surfaces regardless of the underlying Ti composition. Contact-angle measurements on this substrate, when compared to the bulk Ti disks, showed a slightly more hydrophobic surface with an angle of  $63.2^\circ \pm 3.7^\circ$  similar but not identical to literature values, again, owing to the differing cleaning procedures and surface roughnesses.<sup>[41]</sup> However, the effects created by a coating of peptides **12** and **13** were more pronounced than those witnessed earlier with angles of  $8.7^\circ \pm 2.1^\circ$  ( $n=5$ ;  $p < 5 \times 10^{-8}$ ) and  $9.7^\circ \pm 2.9^\circ$ . Again, a slight increase in hydrophobicity was seen with the BSA coating to an angle of  $69.7^\circ \pm 3.0^\circ$ . In order to determine if the contact angle changes were due solely to leaching of the surface-bound molecules into the incident droplets, contact-angle experiments were performed where 30.7  $\mu\text{M}$  concentrations of **12** (0.1 mg mL<sup>-1</sup>) or arginine-glycine-aspartic acid-serine (RGDS) (0.013 mg mL<sup>-1</sup>) were placed onto the surface of a cleaned Ti coated coverslip. Measurements taken show a small decrease in contact angle of  $15.7^\circ \pm 5.6^\circ$  for RGDS and  $11.2^\circ \pm 2.5^\circ$  for **12**, but not the 50° change seen on the peptide-coated surfaces. The concentrations used in this experiment were orders-of-magnitude above the leachable amounts from the surface in coated conditions, and show that the changes in contact angles cannot be due to this effect alone but must also be caused by a change in surface character due to the bound peptide coating.

Next, the cell studies were performed. A 100  $\mu\text{L}$  solution of **12**, **13** (0.1 mg mL<sup>-1</sup> in phosphate buffered saline (PBS)), or plain PBS was added to the center of these slides and let stand for 2 h. The solutions were then removed and 100  $\mu\text{L}$  of a 1% BSA solution was added and the slides were let stand for an additional 2 h. The BSA was removed and the slides were washed with PBS. Next, 100  $\mu\text{L}$  of medium containing  $2.0 \times 10^4$  HUVECs was added and allowed to interact with the surfaces for 60 min. Microscope images were taken of the slides at 0, 15, 30, 45, and 60 min after addition of the cells. After 60 min, the slides were washed profusely with excess PBS and an image was taken of the cells that remained using an actin immunostain. The beginnings of HUVEC spreading can be observed after 15 minutes and is readily apparent after 60 min on the **12** coated (RGD) surface (Fig. 2A and D). In contrast, HUVECs on the **13** (RGE) and uncoated surfaces did not spread as well over the time course of the experiment with only slight pseudopodia observed in most cases (Fig. 2B, C, E, and F). Staining the actin filaments of the cytoskeleton with phalloidin-tetramethyl rhodamine iso-thiocyanate (TRITC) further demonstrates cell spreading on the coated Ti with marked membrane ruffling, and corroborates the differences witnessed with the cells observed in the phase-contrast images (Fig. 2G–I). Surface areas were calculated for 180+ cells in each image revealing that the cells on the uncoated or **13** coated surfaces had approximately identical mean areas at all five time points ( $p > 0.01$ ) and doubled in area during the

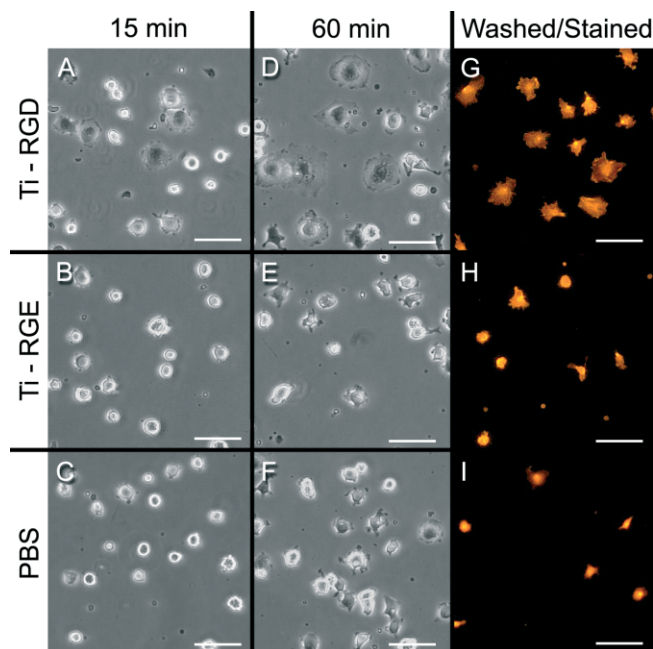


**Figure 2.** Phase contrast image of HUVEC on a Ti-coated glass slide treated with **12** (top), **13** (middle), or PBS (bottom) for 1 h. Images were taken at 15 min (A,B,C), and 60 min (D,E,F) post cell addition, at which point a washing step was performed to remove any unbound cells and actin immunostain was applied (G,H,I) (scale bars in all photos represent 100  $\mu\text{m}$ ).

hour from about 500  $\mu\text{m}^2$  in the initial state to a final size of around 1300  $\mu\text{m}^2$ . Cells of the **12** coated surface rapidly adhered to the surface quadrupling in size over the same hour from about 500  $\mu\text{m}^2$  to a final value of around 2200  $\mu\text{m}^2$ . The surface area of these cells was significantly different than the values for the other conditions at all five time points ( $p < 5 \times 10^{-6}$ ) (Please see Supporting Information Figs. S3 and S4 for further discussion).

After showing that the presence of the RGD motif was responsible for retaining cells on the Ti surface and it was not solely an effect of surface hydrophilicity, where RGE would have performed just as well, the next question to address was whether the binding was too strong thereby negatively affecting migration and proliferation. To assess this possibility, HUVECs were seeded on **12** coated and uncoated Ti disk surfaces and the relative proliferation rate was calculated as follows. Thirty Ti disks were treated with either 1 mg mL<sup>-1</sup> solution of **12** ( $n=15$ ) or buffer ( $n=15$ ) for 1 h at room temperature (RT), and then washed with PBS. BSA was not utilized in this experiment so that attachment rate to the surfaces and spreading rates did not become a factor. Next, 20000 HUVECs in medium were seeded onto ten disks in each group, the other five in each group were exposed to plain media for a background reading. Five of the coated and uncoated disks from each group were immediately developed using an 3(4,5-dimethylthiazol-2-yl)-5-(3-carboxymethoxyphenyl)-2-(4-sulfophenyl)-2H-tetrazolium (MTS) proliferation assay at 1 h. The remaining two groups of five disks were

incubated for 24 h prior to assaying. The proliferation doubling times were determined using an MTS assay and subtracting the background readings from the resultant data points. The proliferation doubling times were found to be  $(25.0 \pm 2.4)$  and  $(22.0 \pm 2.7)$  h for the coated and uncoated Ti surfaces, respectively. The coating did not alter the proliferation of the cells on the surface as the difference between the timings is negligible ( $p = 0.23$ ), and both are within the expected population doubling times reported for HUVECs.<sup>[42,43]</sup>

The above experiments were conducted under static conditions, but many biological processes occur under dynamic conditions, such as flow. Given our interest in endothelialization of metal surfaces and the importance this process has in stenting and ultimate clinical efficacy, we investigated whether this coating affected HUVEC retention under flow. Eight Ti disks were placed in a custom-built flow chamber and treated with either 250  $\mu\text{L}$  of **12** ( $0.1 \text{ mg mL}^{-1}$ ) or 250  $\mu\text{L}$  of PBS for 2 h (Fig. 3A). A 1% BSA solution in PBS was added for an addi-

tion. disks were removed and placed into a 24-well plate. An MTS assay was then used to quantify the number of cells still adhering. Using appropriate controls with known cell counts, we determined that  $(1.5 \pm 0.3) \times 10^4$  cells remained on the uncoated disks, while  $(4.6 \pm 0.2) \times 10^4$  cells remained on the coated surfaces, which is over a 3-fold increase in retention ( $p < 5 \times 10^{-5}$ ). The same 3-fold differential was again witnessed when a 10% serum medium solution was used in place of the 2% serum used earlier ( $p < 5 \times 10^{-4}$ ; Fig. 3B). Even with this relatively short preflow incubation time, the coating increased the cellular binding to the point that almost no cells were lost once the flow began. Additionally, the coating was not affected by the adsorbed proteins such as albumin. The flow rate chosen is at the upper end of venous flow,<sup>[44]</sup> and we are currently designing a system that can simulate arterial flow rates. Importantly, these initial experiments show the benefits of an endothelializing coating to improve cellular attachment under physiological conditions.

In order to confirm integrin-RGD binding was responsible for the attachment difference observed, we performed experiments using soluble tetrapeptide sequences to preblock integrins on the HUVECs. Eight Ti disks were treated with **12** for 2 h followed by 2 h of a BSA block. In the meantime, trypsinized cells were placed into a medium solution supplemented with either 2 mM soluble RGDS or arginine-glycine-glutamic acid-serine (RGES) for 1 h. These treated cells were then placed onto the **12**/BSA-coated Ti disks for 15 min and the flow was started and maintained for 1 h. As before, an MTS assay was used to quantify the number of cells still present on the discs. As shown in Figure 3B, treatment of the HUVECs with RGDS ( $n = 4$ ) prior to placement on the coated Ti disks resulted in a significant decrease in the number of cells adhered, when compared to HUVECs treated with RGES ( $n = 4$ ) ( $p < 5 \times 10^{-4}$ ). Only the soluble RGDS binds to the cell integrin in this modified competitive binding assay. The results of the experiment verify the RGD motif as the primary method through which coating **12** adheres HUVECs. These results are encouraging because integrins are one of the primary methods through which cells receive biological cues from their environment and these specific integrin interactions regulate many aspects of cellular biology. Although, we have initially opted to use the ubiquitous but well-studied RGD domain, more specific endothelial cell binders may be substituted in the future to create a coating with precise phenotype binding control. These studies are ongoing.

In summary, we have designed, synthesized, and characterized a peptide-based implant coating that mediates endothelialization of a synthetic surface. As a prototypical example we examined Ti metal, which lacks a natural ability for directing cellular activity, necessitating surface modification to ensure proper in vivo integration with the surrounding biological matrix. The peptide coating is readily applied to the Ti surface under mild aqueous conditions and shows functionality under dynamic conditions, thereby lending itself to the idea of a prohealing approach to device modification. The materials and methods to coat metal surfaces described herein

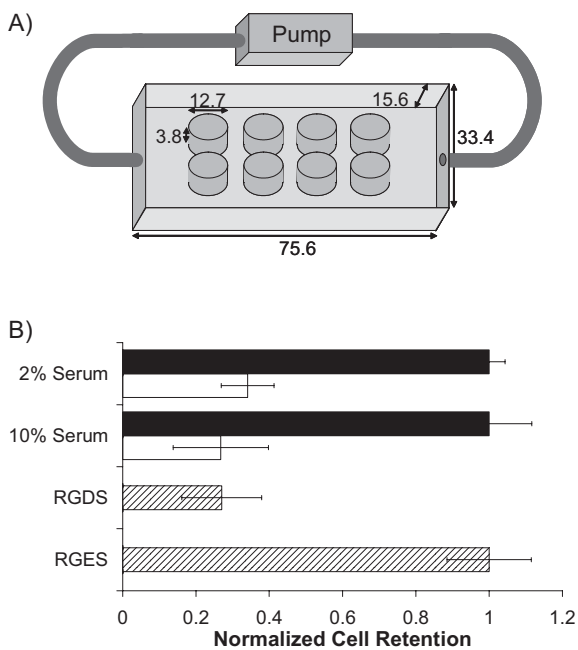


**Figure 3.** A) Top-down schematic of the flow chamber used to evaluate cell attachment under flow conditions. All measurements are in millimeters. B) Flow results for HUVECs under a variety of conditions. Black = **12** coated; white = PBS; diagonal gray = Tetrapeptide pre-incubation with **12** coated surface ( $p < 5 \times 10^{-4}$  for all pairs; error bars indicate standard deviation).

tional 2 h because albumin, a major component of blood, would be present during the attachment process, and is known to block nonspecific binding. The solutions were removed and the disks washed before adding a 250  $\mu\text{L}$  media solution (2% fetal bovine serum (FBS)) containing  $5 \times 10^4$  HUVECs. The cells were allowed to incubate for 15 min before the chamber was filled with medium and the flow started (shear ca.  $5 \text{ dyne cm}^{-2}$ ). The flow was maintained for 1 h at which point the

should be applicable to other medically important metallic surfaces (e.g., stainless steel) and biologics including proteins (e.g., growth factors) and cells (e.g., osteoblasts) because the coating process is mild, can be performed in aqueous solution at neutral pH, and the interfacial coating system is modular with readily interchangeable domains. An interfacial biomaterial coating for a metallic surface (IFBM) that recruits, attaches, and organizes endothelial cells mimics several functions of the ECM, and thus can potentially guide endothelialization on the coated surface. Continued research in this area will foster the development of next-generation biologically inspired tissue-integrated devices for fields ranging from cardiology to implant-based drug delivery.

## Experimental

**Phage Display Metallic Substrates:** Ti 6Al-4V beads of ca. 300  $\mu\text{m}$  in diameter were obtained from Dynamet (Washington, PA). All beads were exhaustively washed in detergent, then rinsed alternately with deionized water and ethanol prior to use. Beads were characterized by using SEM and XPS. SEM showed a smooth bead surface and XPS revealed the presence of a  $\text{TiO}_2$  layer on the surface ( $\text{Ti2p}/\text{O1s}=0.313$ ).

**Ti Disk Manufacture and Cleaning:** Ti disks were lathe cut from a Ti 6Al-4V rod (12.7 mm diameter; 3.8 mm high). Disks were cleaned by first rubbing with 400 grit sandpaper. The disks were then transferred into a beaker containing acetone and shaken for 10 min. This was followed by 10 min of shaking in 95 % ethanol. The disks were then placed into distilled water and cleaned for 20 min (20 % amplitude, 1 s on/1 s off) using an ultrasonic probe (Sonics & Materials, Vibra Cell, Newton, CT). The disks were then placed into a 40 % nitric acid solution for 30 min. Finally, the disks were treated with the ultrasonic tip using the same settings, but for only 10 min, and transferred into a 70 % ethanol holding solution for use in future experiments. Characterization with AFM, SEM, and XPS of the cleaned disks was performed. AFM and SEM analysis showed a surface with roughness of  $\text{rms}\approx 150$  nm, most likely caused by the cutting and subsequent sanding (Fig. S1). XPS analysis showed the presence of a  $\text{TiO}_2$  layer on the surface ( $\text{Ti2p}/\text{O1s}=0.27\pm 0.003$ ) as well as the presence of some surface impurities ( $\text{C1s}/\text{Ti2p}=2.91\pm 0.07$ ).

**Ti Coated Glass Substrates:** Glass microscope slide covers were coated with a 20 nm layer of Ti (cp Ti from Kurt J. Lesker Co., Clairton, PA) by using an e-beam thin-film evaporator (Sharon Vacuum, Brockton, MA). Slides were kept dust free before use and rinsed extensively with ethanol before all studies. Again, XPS, SEM, and AFM studies were performed to examine the surface characteristics of the material. The evaporated Ti surface was both smooth ( $\text{rms}\approx 0.75$  nm) and complete without exposed glass as the Si2p peak did not differ significantly between this surface and the disks used previously ( $p=0.23$ ) (Fig. S1). Additionally, XPS analysis reveals the presence of an oxidized layer ( $\text{Ti2p}/\text{O1s}=0.48\pm 0.01$ ) and a surface relatively free from impurities compared to the disks ( $\text{C1s}/\text{Ti2p}=0.86\pm 0.03$ ).

**Surface Characterization:** Surface characterization of the materials was performed at the Shared Materials Instrumentation Facility at Duke University. AFM (Digital Instruments Dimension 3100) and SEM (FEI XL30 SEM-FEL) were used to examine the surface roughness and topography of the materials. AFM scans were collected in tapping mode using a Veeco silicon probe (TESP). Region scans for disks (30  $\mu\text{m}\times 30$   $\mu\text{m}$  and 10  $\mu\text{m}\times 10$   $\mu\text{m}$ ) and for the Ti-coated coverglass (10  $\mu\text{m}\times 10$   $\mu\text{m}$ ) were collected at a line resolution of  $256\times 256$ . SEM images of Ti-coated coverglass were collected using an electron-beam power of 2 kV (Fig. S1). SEM images of the Ti disk and Ti beads were collected using an electron-beam power of 10 kV (Fig. S1). XPS measurements were performed on a Kratos Analytical

Axis Ultra. Spectra were acquired with a monochromated AlK $\alpha$  X-ray source at a 0-degree take-off-angle, defined as the angle between the surface normal and the axis of the analyzer lens, in the "hybrid" mode with a sampling area of  $700\times 300$   $\mu\text{m}$ . Surface charging was minimized using a low-energy electron flood gun. For each surface, compositional survey scans were collected using a pass energy of 160 eV from three regions. Data has been reported as the average  $\pm$  standard deviation. The software used to analyze the XPS data was CasaXPS version 2.3.12. XPS confirmed the presence of a  $\text{TiO}_2$  coating ( $\text{Ti2p}/\text{O1s}=0.27\pm 0.003$ ) on the 6Al-4V Ti as well as some vanadium and aluminum as expected, with values similar to those reported in the literature acknowledging the slightly different cleaning and passivation strategies used [38].

**Contact-Angle Determination:** The experimental substrate was placed onto the stage of a Kruss DSA 100 contact angle goniometer. Next, a 2.5  $\mu\text{L}$  bead of nanopure water was added and the resulting image was captured and analyzed using drop shape analysis software (Kruss). Reported angles were calculated using a tangential method and averaging the angles from both the left and right sides of the droplet.

**Binding-Affinity Calculations:** Affinity constants were calculated by performing a modified ELISA assay. First, successive dilutions of the biotin-terminated synthesized peptide (1 mg  $\text{mL}^{-1}$  stock in 10 % DMSO/PBS) were made in PBS-T (0.05 % PBS-Tween 20). 100  $\mu\text{L}$  of each dilution was then coated onto the appropriate metal substrate (Ti discs or slides) and incubated at RT for 1 h. After five washes in PBS-T, 100  $\mu\text{L}$  of 1:2500 streptavidin-HRP (Promega) was added to each well and incubated for 1 h at RT. Unbound streptavidin was removed during five PBS-T washes, then the chromogenic substrate ABTS was added and incubated on the bench for 10 min. Supernatants were transferred to a 96-well ELISA plate (CoStar) and the color intensity indicative of bound peptide was measured using a plate reader at 405 nm. A plot of absorbance versus log peptide concentration yielded a sigmoidal plot, the inverse of the half point was used as the affinity constant.

**Phage-Display Libraries:** Metal-binding sequences were identified using a phage-display library developed in-house from phage type M13. The primary library used displayed random peptide sequences on its pIII coat proteins of the format SCX $_{16}$ S, a 19-mer peptide, where X represents one of the twenty naturally occurring amino acids. Each amino acid position was encoded by synthetic NNK codons to somewhat reduce the redundancies in the genetic code.

**Phase Separation Phage Panning of Ti:** In the first round of screening, 25 Ti beads were placed in a 1.4 mL eppendorf tube. 10  $\mu\text{L}$  of the SCX $_{16}$ S library and 200  $\mu\text{L}$  1 % BSA were added to the beads and incubated for 1.5 h with gentle shaking. Next, 400  $\mu\text{L}$  of a 15:1 solution of dibutyl phthalate: cyclohexane (Sigma Aldrich; St. Louis, MO) was added to the phage-bead solution. The tube was inverted several times then rested on the bench to allow phase separation. Both the organic and aqueous phases were removed from the tube, leaving only the Ti beads and strongly bound Ti phage. The phage-bead complexes were transferred to a fresh eppendorf tube and the phage eluted from the beads. Next, 400  $\mu\text{L}$  of concentrated exponential phase TG-1 e-coli cells were added to the solution of phage for the first step in infection. This suspension was incubated at 37  $^\circ\text{C}$  for 30 min, then for 1 h at 37  $^\circ\text{C}$  with shaking. Next, the cell suspension was decanted from the eppendorf into a 15 mL conical tube and incubated for 4 h at 37  $^\circ\text{C}$  with shaking to amplify the phage population. This amplified population was then used as the input for the next round of screening, carried out in an identical fashion to that of the first round. Three such rounds were completed.

**On Phage ELISA:** Freshly amplified phage particles were added to each vials containing the Ti beads. After incubation for 1 h at RT with gentle shaking, HRP-anti-M13 Ab conjugate (Amersham-Pharmacia, Piscataway, NJ), 1:5000 diluted in PBS-T, was then added for 1 h. The vials were washed five times with PBS-T buffer, followed by addition of the substrate ABTS [2,2'-azinobis(3-ethylbenzothiazoline-6-sulfonic acid)] and incubated for 15 min on the benchtop. The absorbance at 405 nm was measured with a Molecular Devices ThermoMax microplate reader.

**Metal-Binding Phage Isolation and Peptide Translation:** Phage from the final rounds of panning were plaque-purified and assayed by ELISA to confirm their binding to the Ti substrate. The DNA of these positive ELISA clones (so labeled due to an absorbance reading at or above 0.500 units) were then isolated using a mini-prep kit (Qiagen) and sequenced following the conventional chain-terminator method.

**Peptide Residue Analysis:** Expected expression levels for the random residue positions were calculated using the reduced genetic code produced by the synthetic NNK codons. Observed frequencies for the 16 variable positions on the 10 Ti binding sequences were tabulated and an expression ratio was calculated (Obs/Exp) for all 20 amino acids (Fig. S2 in Supporting Information).

**Peptide Chemical Synthesis:** Peptides were commercially synthesized by solid-phase peptide synthesis techniques. The resultant peptides were purified to at least 95% purity and included high-performance liquid chromatography and mass spectroscopy analysis. The biotinylated peptide for affinity constant calculation was synthesized using a C-terminal biotin attached through the epsilon amide of a lysine residue.

**Cell Attachment Immunostaining and Phase-Contrast Microscopy:** One Ti-coated glass slide was treated by placing a 100  $\mu\text{L}$  droplet of DPBS in its center, and a second and third slide had a 100  $\mu\text{L}$  droplet of the interfacial coating **12** or **13** (0.1  $\text{mg mL}^{-1}$ ). All slides were left at RT for 2 h. The solutions were removed and the slides were blocked with a 1% BSA solution for an additional 2 h at RT. The BSA solution was removed and the slides were washed with DPBS prior to the addition of 20000 HUVECs in 100  $\mu\text{L}$  EGM-2 medium (Cambrex, system contains 2% serum and a variety of growth factors). The cells were allowed to interact with their respective surfaces for 1 h (37°C, 5% CO<sub>2</sub>) during which time images were taken to show the attachment process. After 1 h, the slides were washed three times with 1 mL PBS-T. 100  $\mu\text{L}$  of a fixative 4% glutaraldehyde solution was added at RT for 20 min. The slides were again washed three times with 1 mL PBS-T. A 100  $\mu\text{L}$  solution of 0.5% Triton X-100 was then added to permeabilize the cells for 20 min at RT. The slides were again washed three times with 1 mL PBS-T. A 1% BSA solution was used to block nonspecific sites for 1 h at 37°C, 5% CO<sub>2</sub>. The slides were washed three times with 1 mL 1% BSA solution. 100  $\mu\text{L}$  of a 1  $\mu\text{g mL}^{-1}$  solution of phalloidin-TRITC conjugate (Sigma) was added and the slides were kept in the dark at RT for 2 h. All unbound phalloidin was washed off using a three times 1 mL 1% BSA wash and images were taken using epifluorescence on an Olympus IX70 microscope with attached charge-coupled device (CCD) camera (Spot Diagnostics 11.2 Color Mosaic).

**Cellular Surface Area Calculation:** Full versions of the images were measured and labeled using ImageJ software (NIH) by drawing a freeform shape around the cell periphery. A total of 182, 200, 220, 204, 191, and 203 cells were used in the determination of the surface areas for the 15 min **12**-coated, 15 min **13**-coated, 15 min uncoated, 60 min **12**-coated, 60 min **13**-coated, and 60 min uncoated images, respectively (Figs. S3, S4 in the Supporting Information).

**Flow-chamber design:** We constructed a custom flow chamber to accommodate the bulk Ti disks used. The chamber and connected pump (peristaltic pump from Fisher) and tubing hold a total volume of around 35 mL of medium and is capable of producing a volume turnover every seven seconds. The setup is capable of holding eight concurrent Ti disks and can subject them to shear flows of around 5  $\text{dynes cm}^{-2}$ .

**Flow Attachment Quantification:** Eight cleaned Ti disks were placed into a dry flow chamber. The disks were treated with either a 250  $\mu\text{L}$  solution of **12** (0.1  $\text{mg mL}^{-1}$  in DPBS) or 250  $\mu\text{L}$  plain DPBS for 2 h. The solutions were removed and 250  $\mu\text{L}$  of a 1% BSA solution was added to the top of each disk for 2 h. The BSA solutions were removed and the disks were washed with 250  $\mu\text{L}$  DPBS. The disks were washed, and upon drying,  $5 \times 10^4$  HUVEC cells were added in 250  $\mu\text{L}$  of EBM-2 medium (Cambrex) supplemented with either 2 or 10% FBS and an array of growth factors. At the same time, control wells were created by placing known cell counts of 0, 2.5, 5, and  $10 \times 10^4$  cells into a 24-well plate with 500  $\mu\text{L}$  of the same medium ( $n = 2$  per

point). After 15 min incubation at RT, 35 mL of medium was added to the chamber and the flow was activated producing a shear force of ca. 5  $\text{dynes cm}^{-2}$  on the surface of the disks. The flow was run continuously for 1 h at which point the medium was removed from the chamber and the disks were quickly moved into empty wells of the control 24-well plate. The wells containing the disks received 500  $\mu\text{L}$  of fresh medium and all wells had 100  $\mu\text{L}$  MTS solution added (Promega CellTiter 96 AQueous One Solution Cell Proliferation Assay). The plate was incubated for 90 min at 37°C, at which point 120  $\mu\text{L}$  aliquots of each well were transferred to a 96-well plate for absorbance reading at 492 nm. The four control points were used to create a conversion factor relating absorbance and cell count ( $R^2 = 0.997$ ). Using this relationship the absorbance readings for the unknown Ti disks and cells was converted to an estimated cell count remaining on the surface.

**Tetrapeptide Competitive Inhibition Assay:** All conditions are identical to the above flow section with the following exception. Before the addition of the cells to the Ti disks, trypsinized cells were added into a tube containing EGM-2 medium (Cambrex, system contains 2% serum and a variety of growth factors) supplemented with 2 mM of RGDS (American Peptide Company; 0.867  $\text{mg mL}^{-1}$ ) or RGEs (American Peptide Company 0.895  $\text{mg mL}^{-1}$ ). Cells and solutions were kept at 37°C for 1 h with occasional brief mixing and then added on top of the coated Ti disks.

**Cell Proliferation Quantification:** HUVECs were cultured using the conditions listed above. Cells were grown to passage three before use. Thirty cleaned Ti disks were treated with either a concentrated 1  $\text{mg mL}^{-1}$  solution of **12** ( $n = 15$ ), or PBS ( $n = 15$ ) for 1 h at RT. The solutions were removed and 10 disks (5 in each treatment) had 200  $\mu\text{L}$  of the plain medium listed above added. The other 20 disks had 20000 cells in 200  $\mu\text{L}$  of the above medium added. The acellular groups, and five in each treatment group of the cellular disks had 40  $\mu\text{L}$  of the MTS assay solution (Promega CellTiter 96 AQueous One Solution Cell Proliferation Assay) added and were incubated for 1 h (37°C and 5% CO<sub>2</sub>). 200  $\mu\text{L}$  aliquots were taken from the disk surface and were put into a polystyrene plate for absorbance reading at 492 nm. The remaining 10 disks were incubated for 24 h before 40  $\mu\text{L}$  of MTS was added, incubated for an additional hour, and aliquots were read on the plater reader. The results from three disks, each from a separate group, could not be determined as the media leaked off of the disks before the aliquots could be taken, leaving a total of 27 usable data points. By subtracting the background readings (acellular disks) from the resultant data points (20000 and unknown cell amounts) and determining the time needed to exponentially double the absorbance reading, and therefore proportionally the cell count, doubling times for the IFBM treated and untreated Ti surfaces were calculated.

Received: January 5, 2007

Revised: May 25, 2007

Published online: August 2, 2007

- [1] B. S. Kim, D. J. Mooney, *Trends Biotechnol.* **1998**, *16*, 224.
- [2] B. Alberts, D. Bray, J. Lewis, M. Raff, K. Roberts, J. D. Watson, in *Molecular Biology of the Cell*, Garland Publishing, New York **1994**, p. 971.
- [3] B. D. Ratner, A. S. Hoffman, F. J. Schoen, J. E. Lemons, *Biomaterials Science: An Introduction to Materials in Medicine*, Academic, San Diego, CA **2000**.
- [4] P. Wu, D. W. Grainger, *Biomaterials* **2006**, *27*, 2450.
- [5] R. Tung, S. Kaul, G. Diamond, P. Shah, *Ann. Intern. Med.* **2006**, *144*, 913.
- [6] F. G. Giancotti, E. Ruoslahti, *Science* **1999**, *285*, 1028.
- [7] B. K. Mann, A. T. Tsai, T. Scott-Burden, J. L. West, *Biomaterials* **1999**, *20*, 2281.
- [8] L. Mazzucchelli, J. B. Burritt, A. J. Jesaitis, A. Nusrat, T. W. Liang, A. T. Gewirtz, F. J. Schnell, C. A. Parkos, *Blood* **1999**, *93*, 1738.
- [9] G. S. Nowakowski, M. S. Dooner, H. M. Valinski, A. M. Mihaliak, P. J. Quesenberry, P. S. Becker, *Stem Cells* **2004**, *22*, 1030.

- [10] D. N. Krag, G. S. Shukla, G. P. Shen, S. Pero, T. Ashikaga, S. Fuller, D. L. Weaver, S. Burdette-Radoux, C. Thomas, *Cancer Res.* **2006**, *66*, 7724.
- [11] W. Arap, R. Pasqualini, E. Ruoslahti, *Science* **1998**, *279*, 377.
- [12] S. Rammelt, T. Illert, S. Bierbaum, D. Scharnweber, H. Zwipp, W. Schneiders, *Biomaterials* **2006**, *27*, 5561.
- [13] J. Schwartz, M. J. Avaltroni, M. P. Danahy, B. M. Silverman, E. L. Hanson, J. E. Schwarzbauer, K. Midwood, E. S. Gawalt, *Mater. Sci. Eng. C* **2003**, *23*, 395.
- [14] T. A. Barber, S. L. Golledge, D. G. Castner, K. E. Healy, *J. Biomed. Mater. Res.* **2002**, *64*, 38.
- [15] D. M. Ferris, G. D. Moodie, P. M. Dimond, C. W. D. Giorani, M. G. Ehrlich, R. F. Valentini, *Biomaterials* **1999**, *20*, 2323.
- [16] S. Tosatti, Z. Schwartz, C. Campbell, D. L. Cochran, S. VandeVondele, J. A. Hubbell, A. Denzer, J. Simpson, M. Wieland, C. H. Lohmann, M. Textor, B. D. Boyan, *J. Biomed. Mater. Res.* **2004**, *68*, 458.
- [17] J. Groll, J. Fiedler, E. Engelhard, T. Ameringer, S. Tugulu, H. A. Klok, R. E. Brenner, M. Moeller, *J. Biomed. Mater. Res.* **2005**, *74*, 607.
- [18] J. Auernheimer, D. Zukowski, C. Dahmen, M. Kantlehner, A. Enderle, S. L. Goodman, H. Kessler, *ChemBioChem* **2005**, *6*, 2034.
- [19] G. P. Smith, V. A. Petrenko, *Chem. Rev.* **1997**, *97*, 391.
- [20] B. K. Kay, J. Winter, J. McCafferty, *Phage Display of Peptides and Proteins*, Academic, San Diego, CA **1996**.
- [21] G. P. Smith, *Science* **1985**, *228*, 1315.
- [22] R. H. Hoess, *Chem. Rev.* **2001**, *101*, 3205.
- [23] J. D. Norris, L. A. Paige, D. J. Christensen, C. Y. Chang, M. R. Huacani, D. Fan, P. T. Hamilton, D. M. Fowlkes, D. P. McDonnell, *Science* **1999**, *285*, 744.
- [24] S. R. Whaley, D. S. English, E. L. Hu, P. F. Barbara, A. M. Belcher, *Nature* **2000**, *405*, 665.
- [25] N. B. Adey, A. H. Mataragnon, J. E. Rider, J. M. Carter, B. K. Kay, *Gene* **1995**, *156*, 27.
- [26] J. de Kruijff, L. Terstappen, E. Boel, T. Logtenberg, *Proc. Natl. Acad. Sci. USA* **1995**, *92*, 3938.
- [27] R. J. Goodson, M. V. Doyle, S. E. Kaufman, S. Rosenberg, *Proc. Natl. Acad. Sci. USA* **1994**, *91*, 7129.
- [28] A. B. Sparks, J. E. Rider, N. G. Hoffman, D. M. Fowlkes, L. A. Quilliam, B. K. Kay, *Proc. Natl. Acad. Sci. USA* **1996**, *93*, 1540.
- [29] A. V. Patwardhan, G. N. Goud, R. R. Koepsel, M. M. Ataai, *J. Chromatogr. A* **1997**, *787*, 91.
- [30] M. Mejare, S. Ljung, L. Bulow, *Protein Eng.* **1998**, *11*, 489.
- [31] S. Brown, *Proc. Natl. Acad. Sci. USA* **1992**, *89*, 8651.
- [32] S. Brown, *Nat. Biotechnol.* **1997**, *15*, 269.
- [33] R. R. Naik, S. J. Stringer, G. Agarwal, S. E. Jones, M. O. Stone, *Nat. Mater.* **2002**, *1*, 169.
- [34] M. Sarikaya, C. Tamerler, A. K. J. Jen, K. Schulten, F. Baneyx, *Nat. Mater.* **2003**, *2*, 577.
- [35] K. I. Sano, K. Shiba, *J. Am. Chem. Soc.* **2003**, *125*, 14234.
- [36] D. J. Kenan, E. B. Walsh, S. R. Meyers, G. A. O'Toole, E. G. Caruthers, W. K. Lee, S. Zauscher, C. A. H. Prata, M. W. Grinstaff, *Chem. Biol.* **2006**, *13*, 695.
- [37] A. B. Sanghvi, K. P. H. Miller, A. M. Belcher, C. E. Schmidt, *Nat. Mater.* **2005**, *4*, 496.
- [38] M. C. Advincula, F. G. Rahemtulla, R. C. Advincula, E. T. Ada, J. E. Lemons, S. L. Bellis, *Biomaterials* **2006**, *27*, 2201.
- [39] Y. J. Lim, Y. Oshida, *Biomed. Mater. Eng.* **2001**, *11*, 325.
- [40] J. Lausmaa, B. Kasemo, *Appl. Surf. Sci.* **1990**, *44*, 133.
- [41] S. R. Sousa, P. Moradas-Ferreira, B. Saramago, L. V. Melo, M. A. Barbosa, *Langmuir* **2004**, *20*, 9745.
- [42] S. C. Thornton, S. N. Mueller, E. M. Levine, *Science* **1983**, *222*, 623.
- [43] T. Shirota, H. Hongbing, H. Yasui, T. Matsuda, *Tissue Eng.* **2003**, *9*, 127.
- [44] A. M. Malek, S. L. Alper, S. Izumo, *JAMA J. Am. Med. Assoc.* **1999**, *282*, 2035.